

PAPER

Asymmetry of the velocity-matching steps in YBCO long Josephson junctions


To cite this article: L S Revin *et al* 2018 *Supercond. Sci. Technol.* **31** 045002

View the [article online](#) for updates and enhancements.

Related content

- [Ferromagnetic resonance with long Josephson junction](#)
I A Golovchanskiy, N N Abramov, V S Stolyarov *et al.*
- [Millimetre and sub-mm wavelength radiation sources based on discrete Josephson junction arrays](#)
M Darula, T Doderer and S Beuven
- [YBa₂Cu₃O₇ long Josephson junctions on bicrystal Zr_{1-x}Y_xO₂ substrates fabricated by preliminary topology masks](#)
D V Masterov, A E Parafin, L S Revin *et al.*

Asymmetry of the velocity-matching steps in YBCO long Josephson junctions

L S Revin^{1,2,3,4}, A L Pankratov^{1,2,3,4} , A V Chiginev^{1,2,4}, D V Masterov¹,
A E Parafin^{1,3} and S A Pavlov¹

¹Institute for Physics of Microstructures of RAS, GSP-105, Nizhny Novgorod, 603950, Russia

²Center of Cryogenic Nanoelectronics, Nizhny Novgorod State Technical University, Nizhny Novgorod, Russia

³Lobachevsky State University of Nizhny Novgorod, Nizhny Novgorod, Russia

⁴National University of Science and Technology MISIS, Moscow, 119049, Russia

E-mail: alp@ipmras.ru

Received 5 June 2017, revised 29 January 2018

Accepted for publication 2 February 2018

Published 19 February 2018



Abstract

We carry out experimental and theoretical investigations into the effect of the vortex chain propagation on the current–voltage characteristics of $\text{YBa}_2\text{Cu}_3\text{O}_{7-\delta}$ (YBCO) long Josephson junctions. Samples of YBCO Josephson junctions, fabricated on 24° [001]-tilt bicrystal substrates, have been measured. The improved technology has allowed us to observe and study the asymmetry of the current–voltage characteristics with opposite magnetic fields (Revin *et al* 2012 *J. Appl. Phys.* **114** 243903), which we believe occurs due to anisotropy of bicrystal substrates (Kupriyanov *et al* (2013 *JETP Lett.* **95** 289)). Specifically, we examine the flux–flow resonant steps versus the external magnetic field, and study the differential resistance and its relation to oscillation power for opposite directions of vortex propagation.

Keywords: YBaCuO Josephson junction, anisotropic high- T_c grain boundary, flux–flow regime, sine-Gordon equation

(Some figures may appear in colour only in the online journal)

1. Introduction

Josephson junctions serve as a suitable media for the study of various soliton dynamics in nonlinear spatially extended systems [1, 2]. Depending on the initial state and external magnetic field various single and multisoliton regimes can be realized in a long Josephson junction [1–3]. While these regimes are now considered to be generally described and understood, recently it has been predicted [4] that in high-temperature junctions, fabricated on bicrystal substrates, a certain asymmetry of flowing currents can appear due to crystallographic anisotropy that can affect the soliton dynamics. The appearance of asymmetry in high- T_c superconducting materials with anisotropic pairing, like cuprates, has been extensively studied from experimental and theoretical points of view. In [5, 6] the inhomogeneity of the critical current density due to the film growth was shown. The strong asymmetry in the displaced linear slope of the YBCO step-edge Josephson junctions was experimentally observed in [7]. In our recent paper [8] we have demonstrated that this

anisotropy can be observed both experimentally and theoretically as the asymmetry of flux–flow steps of current–voltage characteristics (IVCs), but the sample quality at the time did not allow the study of this effect in detail. The investigation of traveling wave (flux–flow) regimes arising in long Josephson junctions is a subject of practical interest for the construction of effective THz sources. In a long junction the mode of dense soliton (fluxon) chain propagation may occur at rather large external magnetic fields in which fluxons are created at one edge of the junction, move along the junction, and are converted into radiation outside the other edge. When the fluxon velocity u approaches the electro-magnetic wave phase velocity \bar{c} , the current–voltage (IV) characteristic will show a current step. This step, often referred as VM step (velocity matching or the flux–flow step), has been observed experimentally [9–14] and theoretically [15–21] mostly for low- T_c Josephson junctions. For high- T_c Josephson junctions there are only a few works about this regime [22–25], and VM steps were not studied for opposite magnetic field signs, assuming symmetric behavior as for short junctions. In a

recent paper [26], the enhancement and asymmetry of VM steps have been shown in a parallel YBCO chain with artificially designed ratched potential.

The aim of this paper is the experimental observation of the asymmetry of flux-flow (velocity-matching) steps for opposite magnetic field directions in the long YBCO grain-boundary junctions (GBJs) and to draw attention to the importance of systematic study of this asymmetry.

2. Experimental setup and theoretical model

The GBJs were fabricated by on-axis dc magnetron sputtering [27] of $\text{YBa}_2\text{Cu}_3\text{O}_{7-\delta}$ thin films on the surface of symmetric $24^\circ (\pm 12^\circ)$ [001]-tilt $\text{Zr}_{1-x}\text{Y}_x\text{O}_2$ bicrystal substrates. The length of the junctions L along the grain boundary varied from 10 to $350 \mu\text{m}$. To obtain better characteristics we have improved the technology and deposited thicker structures of $0.6 \mu\text{m}$ in comparison with the previous samples [8]. In this case we have obtained a significant increase of critical current density values in the range $93\text{--}230 \text{ kA cm}^{-2}$ and the $I_c R_n$ product in the range $0.8\text{--}1.96 \text{ mV}$ for $T = 6 \text{ K}$. The junctions were very long since their lengths are much larger than the Josephson penetration depth $\lambda_J = \sqrt{\Phi_0 / (2\pi\mu_0 J_c d)} = 0.6\text{--}0.9 \mu\text{m}$ ($T \sim 6 \text{ K}$), which determines the size of a fluxon in the junction.

The magnetic field B_e perpendicular to the grain boundary was produced by a current through a copper wire coil, with an inner diameter more than order of magnitude larger than the junction length. Since the junction was placed precisely into the center of the coil, it was assumed that the magnetic field along the junction was nearly uniform. Additional copper heat sinks for the coil were used to prevent heating from the sample at large magnetic fields, and to minimize the bias current overheating, two methods of wire attachment were tried: the bonding of thin wires to the sample and the glueing wires (thicker than in the first case) with silver paste. The second method provides a larger contact area, smaller contact resistance and, therefore, reduces the sample overheating.

The samples were mounted into a pulse tube cryostat and characterized with a precise low-noise current source by standard four-probe technique.

Theoretical analysis was based on the sine-Gordon equation [8]

$$\phi_{tt} + \alpha\phi_t - \phi_{xx} = \beta\phi_{xxt} + \eta(x) - \sin\phi, \quad (1)$$

with dimensionless space and time (normalized to the Josephson length and inverse plasma frequency, respectively), junction length l , normalized bias current distribution $\eta(x)$, damping α and surface loss β parameters. The boundary conditions have the form

$$\begin{aligned} \phi(0, t)_x + \beta\phi(0, t)_{xt} &= \Gamma, \\ \phi(l, t)_x + \beta\phi(l, t)_{xt} &= \Gamma. \end{aligned}$$

Here $\Gamma = H_e / (\lambda J_c)$ is the normalized magnetic field.

While the use of the sine-Gordon equation for modeling of YBCO GBJs is still an open question [28], due to e.g.

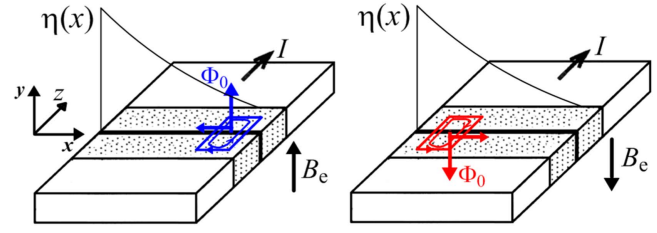


Figure 1. Schematic representation of the fluxon motion along a grain boundary with a nonuniform distribution of the current density $\eta(x)$. Left: accelerating motion of the fluxon from the right to the left boundary with a positive magnetic field B_e . Right: braking motion of the fluxon from the left to the right boundary with a negative magnetic field B_e .

nonsinusoidal current-phase relation [29], detailed investigation of $I_c(\phi)$ for 24° GBJs demonstrated its sinusoidal character [30], and for 32° GBJs the considered model has been successfully used [22].

In the above model (1) we have assumed a nonuniform current distribution $\eta(x)$ due to the GBJ anisotropy [4] with the decay law $\sim \exp(-px)$ (see the inset of figure 4 in [8]). The computer simulations of the sine-Gordon equation are performed for the following parameters: $\beta = 0.1$, α from 1 to 1.5 and junction length $l = 70$.

In figure 1 the schematic designation of the described model is presented. Opposite directions of the magnetic field with the same sign of the bias current lead to the opposite directions of fluxon chain motion along the junction. For the positive B_e , fluxons start to move from the right end with the lower bias current and accelerate under the action of the Lorentz force to the output end, see figure 5 in [31]. In the case of negative B_e , the fluxons are forced to enter, but are not removed effectively.

3. Results and discussion

In [8] long junctions with length $L = 350 \mu\text{m}$ were studied. In the present paper we show that due to improved technology and larger critical currents, the asymmetry of current-voltage characteristics can be visible even for much shorter junctions with length $L = 50 \mu\text{m}$. Such a junction is long in comparison with the Josephson length (about $70 \lambda_J$), because we assume that the anisotropy effect we consider for the [001]-tilt GB is rather weak [4] and the corresponding bias current asymmetry can be detected for long junctions only. Figure 2 (left) shows the experimental IV curves for various values of external magnetic field B_e . We observe field dependent, resonant steps, whose smooth peaks are indicated with arrows (see figure 2). These typical branches are the results of continuous penetration of fluxons from one edge of the junction and propagation to the other [12, 22]. It should be noted that in comparison with Nb junctions [19], for YBCO structures it is rather difficult to distinguish between various step types, such as displaced linear slopes, Fiske steps and VM steps, due to large damping. However, from figure 2 (right) it can be clearly seen that for one magnetic field direction (negative

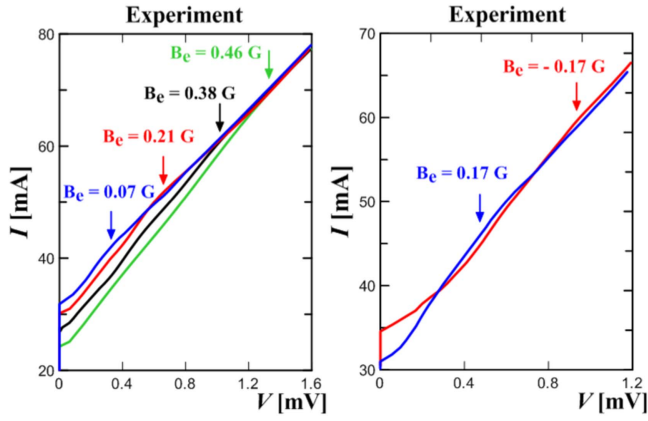


Figure 2. Magnetic field response of bicrystal junction $L = 50 \mu\text{m}$ at $T = 6 \text{ K}$. The maximum heights of the flux-flow steps are indicated with arrows. Left: the experimental IV curves correspond to increasing external magnetic field B_e . Right: the experimental IV curves correspond to the opposite magnetic field directions.

coil current) the VM step is shifted towards the larger voltage and has another slope in comparison with the other direction (positive coil current).

An array of fluxons travels in the junction with phase velocity $u = V_{dc}/(d\mu_0 H_e)$ [22], where V_{dc} is the average voltage across the junction, H_e is the external magnetic field applied in the direction perpendicular to the grain boundary and d is the effective magnetic thickness of the barrier. The voltage corresponding to the top of the flux-flow step in the IV characteristic (arrows in figure 2) is determined by the VM condition: the velocity u approaches the Swihart velocity \bar{c} and, hence, $V_{vm} \approx \bar{c}d\mu_0 H_e = \bar{c}dB_e$. In the literature it is also taken into account that a possible magnetic self-field and the focusing effect of the external magnetic field [32] could make V_{vm} larger. In particular, in [26], VM steps were enhanced due to the use of a discrete parallel array, which leads to the appearance of Cherenkov tails of solitons, interacting with neighbors and synchronizing the soliton chain motion [33], and the ratchet potential, making distinct asymmetry for the direction of soliton motion. In this paper, we study another cause which leads to a shift of the step height V_{vm} maximum. We show that such a shift occurs due to bias current asymmetry, which we believe is associated with the crystallographic anisotropy of bicrystal substrates and hence the asymmetric current flow. The reason is that the regime of fluxon motion from one side to another is expressed more strongly (as a more pronounced VM step) than the regime of motion in the opposite direction. Such a bias current asymmetry can also be due to some random bias current asymmetry for long junctions, but we have observed rather systematic VM step asymmetry for various samples.

The voltage V_{vm} versus the external field for different directions of the fluxon propagation is presented in figure 3. Opposite directions of the magnetic field with the fixed bias current (or the equivalent situation of a fixed magnetic field and oppositely directed current) lead to a different direction of fluxon motion along the junction. In figure 3 (left) the voltage step location $|V_{vm}|$ versus $|B_e|$ is plotted for both cases. It is

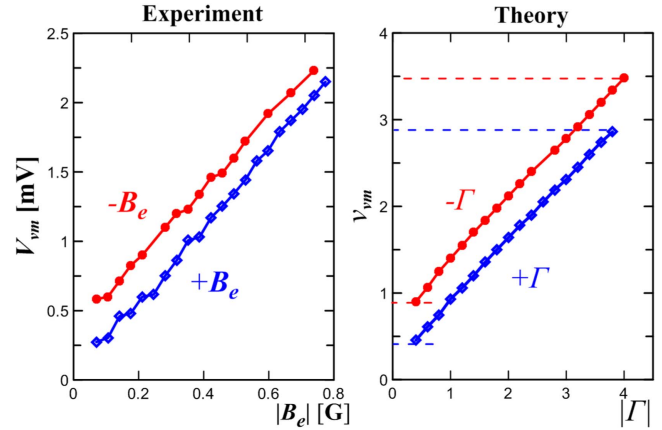


Figure 3. Voltage step depending on magnetic field for bicrystal junction $L = 50 \mu\text{m}$ at $T = 6 \text{ K}$, experiment (left) and theory (right). Opposite directions of fluxon motion are presented.

seen that the dependencies are almost linear with slightly different slopes. Here, the main feature is that the shift of the voltage steps, which are formed by the motion of vortices in one direction, occur at voltages lower than in the case of vortices traveling in the other direction. This means that the optimal generation frequency range, corresponding to VM steps (dashed lines in figure 3), is different for opposite directions of the magnetic field. It is seen that the model characteristics with $\alpha = 1.5$, $l = 70$, $p = 0.0005$ confirm the proposed explanation (figure 3, right). At the maximum temperature of 40 K that we reached in our experiment, the step for a positive magnetic field was still visible, while the step for a negative magnetic field actually disappeared similar to the observation in [26], but there this was at higher temperatures above 77 K.

Another important characteristic of the studied resonance steps is the differential resistance r_d , i.e. the slope of the IV characteristics in the voltage range up to V_{vm} (figure 4, solid curves with symbols, while IVCs are given by short dashed curves). A similar characteristic has been used in [7, 34] to describe the nonresonant fluxon motion with displaced linear slopes appearing in IVCs. In these papers the step amplitude has been plotted for various linear branches, which in our case is equivalent to the plot of differential resistance for various flux-flow branches. It is clearly seen that the sharp increase of r_d corresponds to the position of maximum heights of the flux-flow steps marked V_{vm1} and V_{vm2} . While the IVCs look continuous, there is in fact a jump from the V_{vm} step to the ohmic part of the IVC, which is clearly visible at the differential resistance as its sudden change.

For the considered regime of a continuous flow of fluxons, the most suitable characteristic for the evaluation of Josephson generation is the power P of radiation emitted from the junction output edge. Theoretical analysis provides additional information about the radiation power (figure 5), which is normalized to the Josephson power $P_J = V_J^2/Z_0$, where Z_0 is the characteristic impedance of the junction. The left graph of figure 5 shows the power and r_d for different values of the external magnetic field. It can be seen that the position

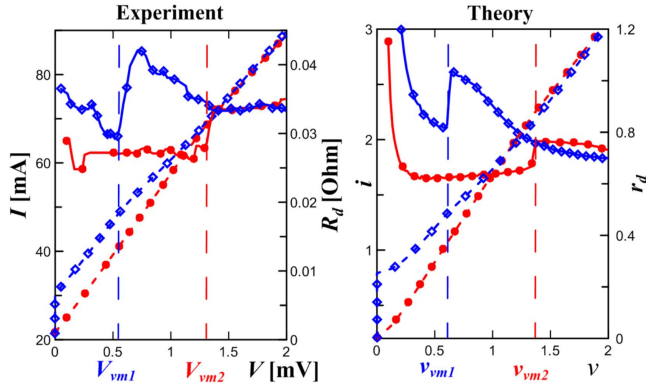


Figure 4. Magnetic field response of bicrystal junction with $L = 50 \mu\text{m}$ at $T = 6 \text{ K}$. Left: the experimental IV curves (dashed) correspond to increased magnetic field $B_e = 0.17 \text{ G}$ (blue with diamonds); $B_e = 0.5 \text{ G}$ (red with circles (left axis)). Right: theoretical i versus v (dashed) for various normalized magnetic field $\Gamma = 0.6$ (blue with diamonds); $\Gamma = 1.6$ (red with circles (left axis)). Solid curves with symbols correspond to the differential resistance r_d (right axis), here symbols are shown for each three to four data points.

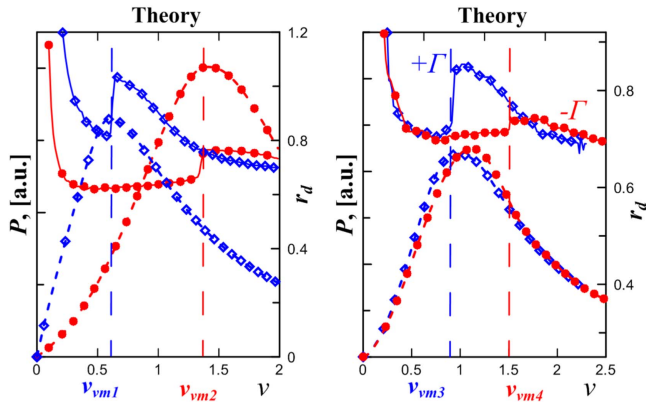


Figure 5. Differential resistance r_d (solid curves with symbols) and output power P (dashed curves with symbols). Left: curves for various normalized magnetic field $\Gamma = 0.6$ (blue with diamonds); $\Gamma = 1.6$ (red with circles). Right: curves for $|\Gamma| = 1$ and opposite directions.

of the step (jump of r_d) for higher magnetic fields is shifted towards higher voltages with a change of the minimum differential resistance. It is also clearly seen that the r_d jump corresponds to the highest output power (v_{vm1} and v_{vm2} voltages in figure 5, left). There is also an assertion about the connection between the step slope (resistance r_d) and the value of electro-magnetic radiation (power P). For low- T_c Josephson junctions, it has been known that the slope of the flux-flow steps influences the output power of generation [12, 31], so for steeper slopes one expects more efficient generation. In this view, enhanced VM steps of asymmetric parallel arrays of [26] must lead to larger generation power. The right graph of figure 5 shows the power and r_d for opposite directions of the external magnetic field with $|\Gamma| = 1$. Values of the minimum differential resistance as well

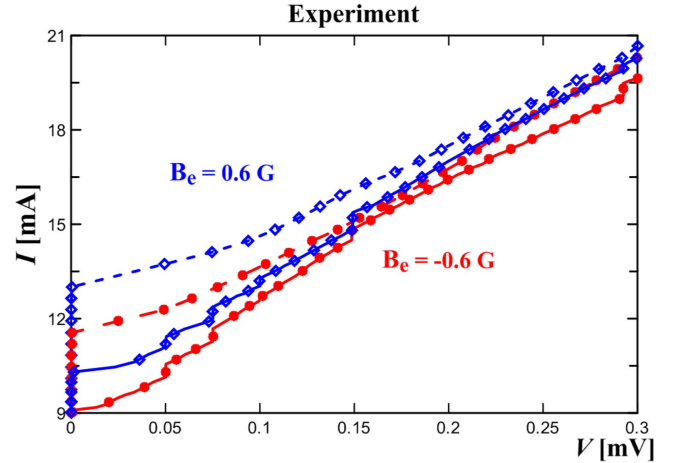


Figure 6. IVCs of the $50 \mu\text{m}$ sample at $T = 6 \text{ K}$ for the external magnetic field $|B_e| = 0.6 \text{ G}$ without ac driving (dashed curves) and under ac driving $f = 72 \text{ GHz}$ (solid curves). Positive B_e is marked by blue diamonds, and the negative by red circles.

as maximum power are almost identical for the two cases, but the step positions are significantly shifted relative to each other according to figure 3. Furthermore, it is seen that the maximum power for the case of $\Gamma = -1$ (red curves) does not match the top of the flux-flow step v_{vm4} , and corresponds to the point below the top. Thus, from differential resistance r_d it is possible to make some predictions about the level of electro-magnetic radiation of the junction, but with care. It is known that the generation frequency is determined by the voltage across the junction by the Josephson relation. Therefore, if one wants to get the maximum of the output power at the frequency $f = 2ev_{vm3}/\hbar$, one needs to use the regime of fluxon motion in one direction (figure 5, blue curve with diamonds). If one is interested in the generation frequency corresponding to the higher voltage v_{vm4} , the maximum radiation corresponds to the opposite fluxon motion (figure 5, red curve with circles).

Another way to observe asymmetry of IVC is to investigate the response of Josephson junctions to the external millimeter-wave radiation. Figure 6 shows the IVCs of a $50 \mu\text{m}$ Josephson junction under the external magnetic field $|B_e| = 0.6 \text{ G}$ with (solid curves) or without (dashed curves) an external signal of frequency $F = 72 \text{ GHz}$. A clearly distinguishable difference in the amplitudes of the first Shapiro steps (at the voltage around 0.15 mV) for opposite directions of the magnetic field indicates different generation regimes with different power at the frequency of the external signal. Here, the Shapiro step amplitude at positive field $B_e = 0.6 \text{ G}$, upper solid curve (blue with diamonds), is twice as large as at the negative field $B_e = -0.6 \text{ G}$, lower solid curve (red with circles). In contrast, at the second Shapiro step (at the voltage below 0.3 mV), due to the change of the maximum of the VM step, and the corresponding change of Josephson generation amplitude, the Shapiro step is much larger at the negative magnetic field than at the positive one. In this experiment we were repeatedly switching the magnetic field (the current

through the coil above the chip) without any change in the external radiation load. Therefore, it is unlikely that the structure receives different power for opposite signs of the magnetic field, but from the general synchronization theory it is known that the synchronization step height is proportional to the product of the amplitudes of the master and slave oscillators. Therefore, the Shapiro step spectroscopy is an effective tool to find the maximum generation amplitude at VM steps without any additional detector. The appearance of multiple fractional Shapiro steps is explained in the literature by either nonsinusoidal current–phase relation or by complex soliton dynamics [35], but will be considered in detail elsewhere.

4. Conclusions

In conclusion, the experimental investigation of flux–flow steps of IV characteristics of long symmetric 24° [001]-tilt $\text{YBa}_2\text{Cu}_3\text{O}_{7-\delta}$ bicrystal grain-boundary junctions has been performed. The effect of the velocity-matching condition has been observed and the strong asymmetry of VM steps has been associated with the asymmetry of bias current distribution. We believe that such bias current asymmetry is due to the anisotropy of the grain-boundary junction on bicrystal substrate, first predicted in [4]. While such bias current asymmetry can also happen as a certain random event for long junctions due to grain-boundary inhomogeneities, we think this effect is less probable due to our new data and rather systematic behavior of the observed effect. However, to fully resolve possible doubts, additional detailed investigations of bias current distribution using a scanning laser method and detailed numerical investigations as in [4] are required, as well as an increase of YBCO grain boundary anisotropy by using underdoped samples. The relationship between the slope of the flux–flow step and the power of the radiation has been studied. It has been demonstrated that the bias current asymmetry does not significantly affect the maximum of the generated power, but allows tuning of the optimal regime of generation by varying the sign of either bias current or external magnetic field. Finally, significant difference of Shapiro step heights at opposite magnetic fields is another way to confirm the asymmetry of generation regimes of YBCO long Josephson junctions.

Acknowledgments

The work is supported by RFBR (project 15-02-05869), by Ministry of Education and Science of the Russian Federation (project 16.2562.2017/PCh), and by NUST MISiS grant K2-2016-051.

ORCID iDs

A L Pankratov  <https://orcid.org/0000-0003-2661-2745>

References

- [1] Likharev K K 1986 *Dynamics of Josephson Junctions and Circuits* (New York: Gordon and Breach) pp 634
- [2] Barone A and Paternò G 1982 *Physics and Applications of the Josephson Effect* (New York: Wiley)
- [3] McLaughlin D W and Scott A C 1978 *Phys. Rev. A* **18** 1652
- [4] Kupriyanov M Y, Khapaev M M, Divin Y Y and Gubankov V N 2012 *JETP Lett.* **95** 289
- [5] Dimos D, Chaudhari P, Mannhart J and LeGoues F K 1988 *Phys. Rev. Lett.* **61** 219
- [6] Bobyl A V, Gaevski M E, Karmanenko S F, Khrebtov I A, Leonov V N, Shantsev D V, Solov'ev V A and Suris R A 1996 *Physica C* **266** 33
- [7] Lombardi F, Scotti di Uccio U, Ivanov Z, Claeson T and Cirillo M 2000 *Appl. Phys. Lett.* **76** 2591
- [8] Revin L S, Chiginev A V, Pankratov A L, Masterov D V, Parafin A E, Luchinin G A, Matrozova E A and Kuzmin L S 2013 *J. Appl. Phys.* **114** 243903
- [9] Zhang Y M, Winkler D and Claeson T 1993 *Appl. Phys. Lett.* **62** 3195
- [10] Koshelets V P, Shchukin A, Lapytskaya I L and Mygind J 1995 *Phys. Rev. B* **51** 6536
- [11] Carapella G, Martucciello N and Costabile G 2002 *Phys. Rev. B* **66** 134531
- [12] Yoshida K, Nagatsuma T, Sueoka K, Enpuku K and Irie F 1985 *IEEE Trans. Magn.* **21** 899
- [13] Ustinov A V, Kohlstedt H and Henne P 1996 *Phys. Rev. Lett.* **77** 3617
- [14] Koshelets V P, Shitov S V, Shchukin A V, Filippenko L V, Mygind J and Ustinov A V 1997 *Phys. Rev. B* **56** 5572
- [15] Nagatsuma T, Enpuku K, Sueoka K, Yoshida K and Irie F 1985 *J. Appl. Phys.* **58** 441
- [16] Zhang Y M and Wu P H 1990 *J. Appl. Phys.* **68** 4703
- [17] Salerno M and Samuelsen M R 1999 *Phys. Rev. B* **59** 14653
- [18] Pankratov A L 2002 *Phys. Rev. B* **66** 134526
- [19] Pankratov A L, Sobolev A S, Koshelets V P and Mygind J 2007 *Phys. Rev. B* **75** 184516
- [20] Jaworski M 2008 *Supercond. Sci. Technol.* **21** 065016
- [21] Jaworski M 2010 *Phys. Rev. B* **81** 224517
- [22] Zhang Y M, Winkler D, Nilsson P-A and Claeson T 1995 *Phys. Rev. B* **51** 8684
- [23] Sung H H, Yang S Y, Horng H E and Yang H C 1999 *IEEE Trans. Appl. Supercond.* **9** 3937
- [24] Winkler D, Zhang Y M, Nilsson P A, Stepantsov E A and Claeson T 1994 *Phys. Rev. Lett.* **72** 1260
- [25] Katterwe S O and Krasnov V M 2011 *Phys. Rev. B* **84** 214519
- [26] Chesca B, John D and Mellor C J 2014 *Supercond. Sci. Technol.* **27** 085015
- [27] Masterov D V, Pavlov S A, Parafin A E and Drozdov Y N 2007 *Tech. Phys.* **52** 1351
- [28] Tafuri F and Kirtley J R 2005 *Rep. Prog. Phys.* **68** 2573
- [29] Il'ichev E, Zakosarenko V, IJsselstein R P J, Hoenig H E, Meyer H-G, Fistul M V and Mueller P 1999 *Phys. Rev. B* **59** 11502
- [30] Golubov A A, Kupriyanov M Y and Il'ichev E 2004 *Rev. Mod. Phys.* **76** 411
- [31] Matrozova E A, Revin L S and Pankratov A L 2012 *J. Appl. Phys.* **112** 053905
- [32] Nagatsuma T, Enpuku K, Yoshida K and Irie F 1984 *J. Appl. Phys.* **56** 3284
- [33] Soloviev I I, Klenov N V, Pankratov A L, Il'ichev E and Kuzmin L S 2013 *Phys. Rev. E* **87** 060901(R)
- [34] Cirillo M, Merlo V and Gronbech-Jensen N 1999 *IEEE Trans. Appl. Supercond.* **9** 4137
- [35] Terpstra D, IJsselstein R P J and Rogalla H 1995 *Appl. Phys. Lett.* **66** 2286